Noninvasive MRI-Based Liver Iron Quantification: Methodic Approaches, Practical Applicability and Significance

Nicht invasive MRT-basierte Bestimmung des Leber-Eisen-Gehalts: Methodische Ansätze, Anwendbarkeit in der Praxis und Aussagekraft

Authors A. P. Wunderlich[1,4], H. Cario[2], M. S. Juchems[3], M. Beer[4], S. A. Schmidt[4]

Affiliations
[1] Section for Experimental Radiology, Universitätsklinikum Ulm, Germany
[2] Department of Pediatrics and Adolescent Medicine, Universitätsklinik Ulm, Germany
[3] Diagnostic and Interventional Radiology, Konstanz Hospital, Konstanz, Germany
[4] Clinic for Diagnostic and Interventional Radiology, Universitätsklinikum Ulm, Germany

Key words
- abdomen
- MR-imaging
- iron

Abstract

Due to the dependence of transverse relaxation times T_2 and T_2^* on tissue iron content, MRI offers different options for the determination of iron concentration. These are the time-consuming spin-echo sequence as well as the gradient-echo sequence. For the latter, several data analysis approaches have been proposed, with different requirements for acquisition and post-processing: the mathematically challenging R_2^* analysis and the signal-intensity ratio method with its high demand on the signal homogeneity of MR images. Furthermore, special procedures currently under evaluation are presented as future prospects: quantitative susceptibility imaging, as a third approach for analyzing gradient echo data, and multi-contrast spin-echo using repeated refocusing pulses. MR theory, as far as needed for understanding the methods, is briefly depicted.

Key points:
- Description of underlying technology of different MRI-based procedures for liver iron quantification
- Applicability of these methods in clinical practice
- Validity of the methods, i. e. positive and negative predictive value, if available

Citation Format:
- Wunderlich AP, Cario H, Juchems MS et al. Noninvasive MRI-Based Liver Iron Quantification: Methodic Approaches, Practical Applicability and Significance. Fortschr Röntgenstr 2016; 188: 1031–1036

received 27.10.2015
accepted 29.7.2016

Bibliography
DOI http://dx.doi.org/10.1055/s-0042-115570
Published online: 14.9.2016
Fortschr Röntgenstr 2016; 188: 1031–1036 © Georg Thieme Verlag KG Stuttgart · New York · ISSN 1438-9029

Correspondence
Dr. Arthur P. Wunderlich
Klinik für Diagnostische und Interventionelle Radiologie,
Universitätsklinikum Ulm
Albert-Einstein-Allee 23
D-89070 Ulm
Germany
Tel.: ++ 49/7 31/50 06 10 86
Fax: ++ 49/7 31/50 06 11 08
arthur.wunderlich@uni-ulm.de

Zusammenfassung

Aufgrund des Einflusses des Gewebe-Eisengehalts auf die transversalen Relaxationszeiten T_2 und T_2^* bietet die MRT verschiedene Möglichkeiten zur In-vivo-Bestimmung der Eisenkonzentration. Dies sind im Einzelnen die zeitaufwändige Spin-Echo- sowie die Gradienten-Echo-Methode. Bei Letzterer gibt es prinzipiell mehrere Ansätze zur Datenauswertung, mit unterschiedlichen Voraussetzungen für Aufnahmetechnik und Nachverarbeitung: Einerseits die mathematisch anspruchsvolle R_2^*-Analyse, andererseits das Signalintensitätsverfahren, das hohe Anforderungen an die Signalhomogenität der MRT-Bilder stellt. Darauf aufbauende bzw. weiterführende Methoden sind: Die quantitative Suszeptibilitäts-Bestimmung als dritter Ansatz zur Auswertung von Gradienten-Echo-Daten, sowie die Multi-Kontrast Spin-Echo-Technik mit wiederholten Refokussierungspulsen. Die Theorie der MRT, sofern für das Verständnis der Methoden notwendig, wird in aller Kürze beleuchtet.

Pathophysiology of iron overload

Normal iron content plays an important role in the physiological processes of the human body. A disturbance to the precisely regulated iron metabolism system has serious consequences. Therefore, for example, iron overload results in oxidative damage to membrane lipids and proteins and in DNA damage that can cause mitochondrial and lysosomal dysfunction, changes in gene expression, and changes in tumor suppressor genes (p53). Organ damage due to iron overload primarily affects the heart and liver as well as the endocrine organs, i. e., the pituitary gland, pancreas, thyroid, parathyroid, and gonads [1]. Cardiac insufficiency and arrhythmia as a result of myocardial siderosis are the most

common causes of death in patients with transfusion-related iron overload [2]. The growth of hepatocellular carcinomas following hepatic siderosis often with a hepatitis C infection as an additional pathogenetic factor has become increasingly important in recent years [3].

As an example, Hernando and Wood provide an overview of the mechanisms of iron overload [4, 5]. Both hereditary and acquired factors can result in iron overload (primary and secondary hemochromatosis). The various forms of hereditary hemochromatosis cause disruption of the hepcidin-dependent regulation of iron absorption [6]. As a result of suppression of hepcidin synthesis, anemias with greatly increased but ineffective erythropoiesis (e. g. thalassemia intermedia, congenital dyserythropoietic anemia, MDS) also result in increased iron absorption via the intestinal mucosa and thus in secondary hemochromatosis [6]. The most important cause of secondary hemochromatosis is parenteral iron intake via blood transfusion, e. g. in the case of thalassemia major or other chronic types of anemia.

Early and precise diagnosis of iron overload is essential for the initiation of iron elimination therapy in a timely manner. In contrast to hereditary hemochromatosis in which iron removal is performed via phlebotomy, chelate therapy with medication is indicated here with a few exceptions (after stem cell transplantation, individual cases of congenital dyserythropoietic anemia). At present, the most important medication is deferasirox, which is approved for the treatment of both transfusion-related and absorption-related iron overload in thalassemia intermedia. Due to the side effects, primarily nephrotoxicity and hepatotoxicity, overtreatment must be avoided. For detailed information regarding iron elimination, refer to the corresponding overviews and guidelines [7].

In summary, quantification of the non-heme iron stores must be exact as possible because this is necessary both for confirming diagnosis and for monitoring therapy. Serum ferritin concentrations can be easily determined in daily routine, but are only conditionally reliable since serum ferritin as an acute phase protein is altered in inflammatory reactions and in different liver diseases as well [8]. Moreover, it is known, for example, that the serum ferritin concentration in patients with thalassemia intermedia is significantly lower than the values to be expected in relation to the total body iron load [9]. The liver iron concentration is suitable for the exact assessment of the total body iron load since it is correlated in a linear fashion with the iron load of the organism. The previously routinely performed determination of iron content via liver biopsy is invasive and associated with a relevant risk of complications. In addition, the iron distribution within the liver parenchyma is usually particularly inhomogeneous [10] so that a biopsy is not necessarily representative for the entire organ [11]. This resulted in a search for other precise and ideally noninvasive methods.

History of liver iron content determination via MRI

With the introduction of MRI in the clinical routine, an effect of the liver iron content on the MR signal was identified [12, 13]. The first systematic studies on this topic [14 – 17] that qualitatively correlated the liver MRI signal with varying degrees of iron overload were published more than twenty years ago. Based on the studies of Alustiza, Gandon and St. Pierre, quantitative determination of liver iron content has been possible for ten years [18 – 20]. Yokoo et al. provide an overview of this development [21]. Today MR-based methods for determining liver iron content are an essential part of guideline recommendations for managing secondary iron overload [7] (latest version available at: http://www.awmf.org/leitlinien/detail/ll/025 – 029.html).

However, a recently published meta-analysis came to a very sobering conclusion regarding the diagnostic accuracy of MRI-based liver iron quantification: Sarigianni et al. determined negative and positive predictive values of only approx. 0.8 depending on the method [22]. This means that with the available methods an iron overload is overlooked or underestimated in approx. 20 % of patients while inappropriate therapeutic conclusions with the risk of therapy-associated side effects are drawn in a comparably sized group of patients based on false-positive findings.

The goal of this study is to present the approaches of the different methods. The validity of the individual methods is discussed and weaknesses that may be reasons for limited clinical significance are described. Finally, the practical applicability of the methods is discussed.

Basic MR theory

In all of the methods described in the following, liver iron content is determined based on the transverse relaxation rate, the inverse of the transverse relaxation time characterizing the MR signal decay. This signal decay is comprised of an irreversible component R_2 primarily due to spin-spin relaxation. In addition, there is a reversible component R_2' resulting from dephasing of the nuclear spins of hydrogen atoms. This is caused by different magnetic fields at the site of the nucleus of the hydrogen atom due to chemical bonds (C-H bond in fat, O-H bond in water) which then result in precession at different Larmor frequencies. The impairment of magnetic field homogeneity due to local differences in magnetic susceptibility of different tissue with accordingly differing Larmor frequencies of the atomic nuclei is also a factor. This effect is particularly pronounced as a result of hemosiderin deposits in the liver, particularly in the case of increased iron content.

In spin-echo sequences, spin dephasing is reversed by the refocusing pulse so that only the irreversible component of the transverse relaxation rate, i. e., R_2, is observed. This refocusing is eliminated in the gradient-echo method so that both components have an effect and the transverse relaxation rate is the sum of R_2 and R_2', referred to as R_2^* for short. This is the inverse of the characteristic transverse relaxation time for gradient echo T_2^*.

The MRI method in detail

Spin-echo sequence

Historically used first [12, 13], this method was then further developed by St. Pierre [20] on the basis of the data of 40 patients into a validated, FDA-approved, CE-certified, fee-based method under the name Ferriscan®. The method is

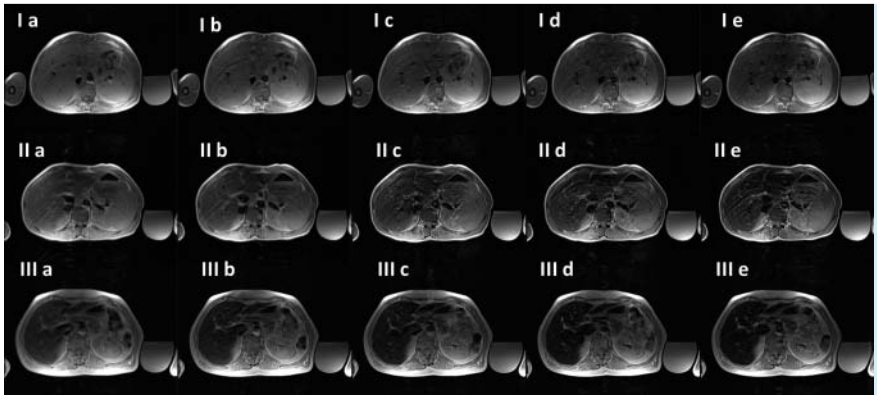

Fig. 1 Spin-echo images at different echo times. Columns **a-e**: TE = 6 -9- 12 -15- 18 ms. Upper row (I): Pat. 1 with nearly normal liver iron content (47 µmol/g, all values given in liver dry weight). Middle row (II): Pat. 2 with a liver iron content of 107 µmol/g, showing need for therapy which is indicated above a level of 80 µmol/g. Lower row (III): images of Pat. 3 with 281 µmol/g liver iron content, which is below the threshold of 360 µmol/g pointing to a risk of severe organ siderosis. Signal attenuation with increasing TE, which is more prominent at a higher liver iron content, is clearly visible.

based on the fact that the liver signal decreases as the echo time (TE) increases as shown in ◉ **Fig. 1**. Subsequent revalidation of the method on the basis of 223 patients [23] showed a certain range of the results with an average deviation compared to liver biopsy of 35 %. In contrast to the non-linear relationship between R_2 and liver iron content in a range of up to 40 mg/g dry weight stated in the studies by St. Pierre et al. [20, 23], Wood showed a linear course (as is theoretically to be expected), but only for a maximum liver iron concentration of up to 30 mg/g dry weight (fig. 2 in ref. [17]). However, due to the range, the values are not significantly different (ref. [17], ◉ **Fig. 3**).

In spin-echo, individual echoes must be recorded, i. e., the multiple measurements needed to determine the R_2 relaxation rate at different echo times may not be performed after a single excitation as in multi-contrast spin-echo (see below) but rather a separate measurement is required for each of the five echo times. This causes the scan time of over 16 minutes needed for the Ferriscan® method.

After MRI examination, the data are sent online and the result is typically available within one workday. Scanners must be calibrated every 18 months. The same protocols as used for patient examinations are to be recorded using a phantom – a total time expenditure of approx. half an hour. Each examination incurs a cost of several hundred Euros to be negotiated for each operator.

The already mentioned meta-analysis by Sarigianni et al. specifies a positive predictive value of 0.81 and a negative predictive value of 0.83 for the spin-echo method [22].

Gradient-echo sequence

The majority of published studies are based on this method. The advantage of this method is the shorter scan time so that the necessary data can be acquired during breathhold. Moreover, signals with different echo times can be repeatedly read out after a single excitation (multi-contrast technique, see [24], for example). The following describes the various ways in which the liver iron content is determined from the image data. There are essentially three approaches: a) Determination of the hepatic R_2^* relaxation rate, b) Calculation of the ratio of the signals from liver tissue and reference tissue, and c) Determination of magnetic susceptibility.

For all gradient-echo analysis methods together, Sarigianni et al. specifies a positive predictive value of 0.88 and a negative predictive value of 0.74 [22]. The latter is probably due to the large range of R_2^* values in normal persons [25].

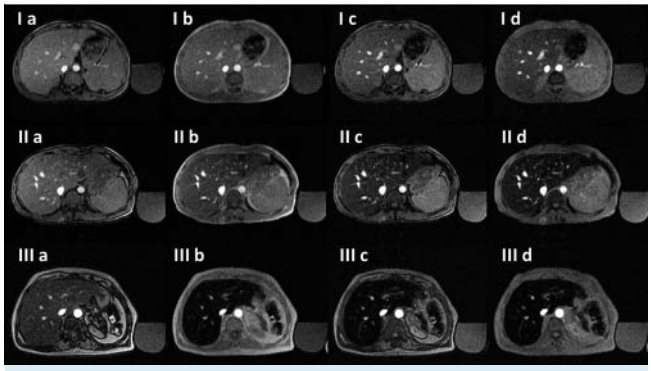

Fig. 2 Gradient-echo images of the three patients shown in Fig. 1. Columns a-d: TE = 2.38 – 4.76 – 7.14 – 9.52 ms. These echo times correspond to those specified as in-phase (columns **b**, **d**) and opposed-phase (**a**, **c**) for the scanner employed (Siemens Avanto, 1.5 T). Opposed-phase images show a delineation between subcutaneous fat and muscle tissue below, which doesn't appear on in-phase images (columns **b** and **d**). Furthermore, signal attenuation with growing TE is evident, which again increases with greater iron overload (row I-III).

Relaxation rate R_2^*

Because of the different precession frequencies of fat and water, an effect corresponding to the acoustic phenomenon known as "beat" is observed: If two minimally different frequencies are mixed, an increasing and decreasing volume is perceived. In MRI this means that the sum (in-phase) or the difference (opposed-phase) of the fat and water signals is displayed depending on the echo time (TE), see ◉ **Fig. 2**. For tissue containing both water and fat, the signal therefore does not attenuate in a monotone manner with an increasing TE but rather shows minimums for opposed-phase TEs and maximums for in-phase TEs. Since different echo times are also necessary in the gradient-echo method for the determination of transverse relaxation rate R_2^*, this behavior must be taken into consideration to prevent incorrect results in the case of possible steatosis [26 – 28].

The fat signal is composed of multiple components with varying Larmor frequencies [29]. This means that the above description of the in-phase and opposed-phase effect is a simplification. Even restriction to in-phase echo times with fit to a monoexponential decay curve does not allow reliable determination of R_2^* [30]. The influence of fat components must therefore always be taken into consideration.

Despite this, almost all studies [16, 17, 31 – 37], with a few exceptions [27, 38, 39], determine transverse relaxation

rate R_2^* by fitting to an exponential curve analogously to the procedure that is appropriately used for the determination of R_2 in the case of spin-echo data. This is possibly the reason for the dependence of the consistency of results on the minimum echo time as postulated by Henninger et al. [36]. The attempt to substantiate the plausibility of the observed results with mathematic simulations of the MR signal [40] is of limited value since the simulation method does not take the influence of the described dephasing between the fat signal and water signal into consideration.

Although the determination of R_2^* under consideration of the influence of fat is mathematically complicated, the result can be calculated within several minutes once the parameters have been programmed. Major manufacturers provide options for the immediate creation of R_2^* parameter maps in the program so that the result is available directly on the scanner. Therefore, the total time spent is minimal. However, systematic studies regarding iron quantification using R_2^* values in larger patient populations are not yet available.

Signal-intensity ratio

The signal intensity of liver tissue in relation to fat tissue or skeletal muscles is determined. Since this ratio depends on the R_2^* value of the liver with a defined echo time, it is also suitable for determining liver iron content.

The method was applied for the first time by Hernandez et al. [14] to gradient-echo sequences. A further development of the method was published by Gandon et al. [19]. Gandon's method is based on the postulated linear relationship between the LIC and signal intensity ratio (SIR) depending on the protocol. It is available free of cost via a web interface, is relatively widely used, and is sometimes called the SIR method although alternatives to the analysis of the SIR values used by Gandon are conceivable [18]. A comparison between Gandon's approach and the Ferriscan® method showed a discrepancy in the results, namely a significant overestimation of the LIC in the range of 50 – 300 µmol/g (3 – 17 mg/g) [41]. Follow-up is only conditionally possible with this method. The LIC overestimation, particularly in the range around 80 µmol/g (4.5 mg/g) that is important for treatment management, will often result in overtreatment. Deviations of the method publicized by Gandon from R_2^*-based methods were also observed [31, 42].

Gandon's method is limited to a maximum liver iron content of 350 µmol/g (20 mg/g) which is often exceeded particularly in patients receiving regular transfusions. This prompted the add-on proposed by Rose et al. [43]. By using shorter echo times, it is possible to quantify even extreme iron overload, however, with the risk of overestimation of the iron concentration if fatty degeneration of the liver is also present.

Mathematic determination of signal intensities and their ratio is very simple. The described discrepancies between Gandon's method and the Ferriscan method cannot be explained by shortcomings of the method. A suitable evaluation of the signal intensity ratio via its natural logarithm, called the SIR Using Logarithm of Median ROI Values, SIR-ULM for short, allows reliable determination of liver iron content at 3 Tesla with a positive and negative predictive value of 0.9 and 0.93, respectively, for the threshold of 125 µmol/g (7 mg/g) dry weight used in the meta-analysis [44].

Susceptibility

The local magnetic field strength, which depends on the iron content, can be determined from a corresponding analysis of the MRI signals [45]. A comparison with reference tissue makes it possible to determine the magnetic susceptibility of the tissue in question, i. e., the amplification of the external magnetic field primarily caused by the iron that is present [46]. After corresponding calibration, the susceptibility value can then be used to determine the iron concentration. In contrast to transverse relaxation times, this biomarker is dependent on the field strength that is used.

Multi-contrast spin-echo sequence

After data acquisition in spin-echo, additional refocusing can be performed by applying 180° pulses so that images can be acquired with additional echo times. However, in inhomogeneous tissues such as the liver, refocusing is only effective in the case of stationary hydrogen atoms. The time between refocusing pulses, known as echo spacing, influences the amount of time during which movement of hydrogen atoms affects the MRI signal. The dependence of the signal intensity on the time interval of the recorded echoes is described based on theoretical observations [47]. Examples are shown in **Fig. 3**. Jensen et al. were able to show that it is possible to differentiate between dissolved iron (associated with ferritin by the authors) and the aggregated form (hemosiderin) with the acquisition of multiple series with different echo intervals [48]. The sum of the two components results in more precise determination of liver iron content than each individual component. The following should be noted: the results acquired by Jensen on the basis of a phantom indicate that the R_2 relaxation rate determined using spin-echo does not correlate significantly with the concentration of dissolved iron or of hemosiderin [48]. The correlation of R_2 to the total iron content is also only moderate. However, gradient-echo data, i. e., the R_2^* relaxation rate, shows a good correlation with the hemosiderin concentration and a relatively good correlation with the total iron concentration [48].

The multi-contrast spin-echo method was used by Tang et al. in patients with iron overload [49]. Good agreement between the total liver iron content determined by MRI and biopsy was seen. Only the subjects without iron overload in Tang's study were taken into consideration in the meta-analysis mentioned above [22] since the patient group did not meet the inclusion criteria of the meta-analysis.

Conclusion and outlook

MRI is a noninvasive, readily available method for the quantification of liver iron content. In contrast to biopsy which can result in a significant sample error [11], the majority of the liver is scanned via MRI so that it is possible to determine the total iron content [50] and to draw conclusions regarding focally increased or reduced accumulation. The variability of the iron content of liver biopsies [11] calls the reliability of the gold standard into question [25].

There are a number of studies on the determination of liver iron content via MRI with a substantial majority using the gradient-echo technique with determination of the transverse relaxation rate R_2^*. Unfortunately, an adequate analy-

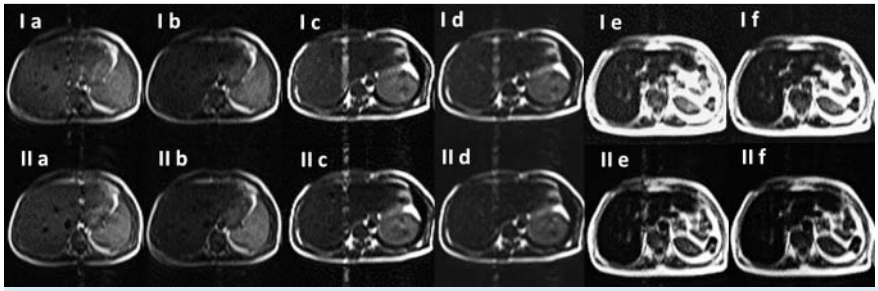

Fig. 3 Multi-contrast spin-echo images of the three patients depicted in Fig. 1 with different echo times and different echo spacing. Columns **a, c**, and **e**: TE = 8 ms, **b**, **d** und **f**: TE = 16 ms. Row I: echo spacing 4 ms, row II: echo spacing 8 ms. Columns **a** and **b** show pat. 1, **c** and **d** show pat. 2, and **e** and **f** show pat. 3. Besides the influence of echo time, the effect of echo spacing becomes evident (row I vs. II), which is barely visible in pat. 1 but shows increasing impact with increasing iron content and in pat. 3 predominates the signal loss due to prolonged TE.

sis method with consideration of the liver fat content has only been insufficiently evaluated to date.

The analysis of signal ratios between the liver and reference tissue according to Gandon [19] is apparently problematic [31, 41, 42]. A further approach introduced by Alustiza that also uses the signal ratio [18] has received little attention. A new analysis method based on SIR allows reliable determination of liver iron content at 3 Tesla [44].

In conclusion, the majority of existing MRI-based methods for liver iron quantification currently only have moderate positive and negative predictive values. This study shows some approaches for providing fundamental improvements. The extent to which methodic improvements in data analysis for established methods (gradient-echo) or completely new MRI concepts (multi-contrast spin-echo) can contribute to a further increase in significance remains to be seen.

References

1 *Wood JC*. History and current impact of cardiac magnetic resonance imaging on the management of iron overload. Circulation 2009; 120: 1937 – 1939
2 *Borgna-Pignatti C*, *Cappellini MD*, *De Stefano P et al.* Survival and complications in thalassemia. Annals of the New York Academy of Sciences 2005; 1054: 40 – 47
3 *Borgna-Pignatti C*, *Garani MC*, *Forni GL et al.* Hepatocellular carcinoma in thalassaemia: an update of the Italian Registry. British journal of haematology 2014; 167: 121 – 126
4 *Hernando D*, *Levin YS*, *Sirlin CB et al.* Quantification of liver iron with MRI: state of the art and remaining challenges. JMRI 2014; 40: 1003 – 1021
5 *Wood JC*. Estimating tissue iron burden: current status and future prospects. British journal of haematology 2015; 170: 15 – 28
6 *Steinbicker AU*, *Muckenthaler MU*. Out of balance – systemic iron homeostasis in iron-related disorders. Nutrients 2013; 5: 3034 – 3061
7 *Cario H*, *Grosse R*, *Janssen G et al.* Guidelines for diagnosis and treatment of secondary iron overload in patients with congenital anemia. Klinische Padiatrie 2010; 222: 399 – 406
8 *Puliyel M*, *Sposto R*, *Berdoukas VA et al.* Ferritin trends do not predict changes in total body iron in patients with transfusional iron overload. American journal of hematology 2014; 89: 391 – 394
9 *Taher AT*, *Musallam KM*, *Wood JC et al.* Magnetic resonance evaluation of hepatic and myocardial iron deposition in transfusion-independent thalassemia intermedia compared to regularly transfused thalassemia major patients. American journal of hematology 2010; 85: 288 – 290
10 *Ghugre NR*, *Coates TD*, *Nelson MD et al.* Mechanisms of tissue-iron relaxivity: nuclear magnetic resonance studies of human liver biopsy specimens. MRM 2005; 54: 1185 – 1193
11 *Emond MJ*, *Bronner MP*, *Carlson TH et al.* Quantitative study of the variability of hepatic iron concentrations. Clinical chemistry 1999; 45: 340 – 346
12 *Stark DD*, *Moseley ME*, *Bacon BR et al.* Magnetic resonance imaging and spectroscopy of hepatic iron overload. Radiology 1985; 154: 137 – 142
13 *Brasch RC*, *Wesbey GE*, *Gooding CA et al.* Magnetic resonance imaging of transfusional hemosiderosis complicating thalassemia major. Radiology 1984; 150: 767 – 771
14 *Hernandez RJ*, *Sarnaik SA*, *Lande I et al.* MR evaluation of liver iron overload. JCAT 1988; 12: 91 – 94
15 *Rocchi E*, *Cassanelli M*, *Borghi A et al.* Magnetic resonance imaging and different levels of iron overload in chronic liver disease. Hepatology 1993; 17: 997 – 1002
16 *Anderson LJ*, *Holden S*, *Davis B et al.* Cardiovascular T_2-star (T_2^*) magnetic resonance for the early diagnosis of myocardial iron overload. European heart journal 2001; 22: 2171 – 2179
17 *Wood JC*, *Enriquez C*, *Ghugre N et al.* MRI R_2 and R_2^* mapping accurately estimates hepatic iron concentration in transfusion-dependent thalassemia and sickle cell disease patients. Blood 2005; 106: 1460 – 1465
18 *Alustiza JM*, *Artetxe J*, *Castiella A et al.* MR quantification of hepatic iron concentration. Radiology 2004; 230: 479 – 484
19 *Gandon Y*, *Olivie D*, *Guyader D et al.* Non-invasive assessment of hepatic iron stores by MRI. Lancet 2004; 363: 357 – 362
20 *St Pierre TG*, *Clark PR*, *Chua-anusorn W et al.* Noninvasive measurement and imaging of liver iron concentrations using proton magnetic resonance. Blood 2005; 105: 855 – 861
21 *Yokoo T*, *Browning JD*. Fat and iron quantification in the liver: past, present, and future. Topics in magnetic resonance imaging 2014; 23: 73 – 94
22 *Sarigianni M*, *Liakos A*, *Vlachaki E et al.* Accuracy of magnetic resonance imaging in diagnosis of liver iron overload: a systematic review and meta-analysis. Clinical gastroenterology and hepatology 2015; 13: 55 – 63 e55
23 *St Pierre TG*, *El-Beshlawy A*, *Elalfy M et al.* Multicenter validation of spin-density projection-assisted R_2-MRI for the noninvasive measurement of liver iron concentration. MRM 2014; 71: 2215 – 2223
24 *Chandarana H*, *Lim RP*, *Jensen JH et al.* Hepatic iron deposition in patients with liver disease: preliminary experience with breath-hold multiecho T_2^*-weighted sequence. Am J Roentgenol 2009; 193: 1261 – 1267
25 *Hope TA*, *Ohliger MA*, *Qayyum A*. MR imaging of diffuse liver disease: from technique to diagnosis. Radiologic clinics of North America 2014; 52: 709 – 724
26 *Ghugre NR*, *Enriquez CM*, *Coates TD et al.* Improved R_2^* measurements in myocardial iron overload. JMRI 2006; 23: 9 – 16
27 *Hernando D*, *Kramer JH*, *Reeder SB*. Multipeak fat-corrected complex R_2^* relaxometry: theory, optimization, and clinical validation. MRM 2013; 70: 1319 – 1331
28 *Sirlin CB*, *Reeder SB*. Magnetic resonance imaging quantification of liver iron. Magnetic resonance imaging clinics of North America 2010; 18: 359 – 381, ix
29 *Hamilton G*, *Yokoo T*, *Bydder M et al.* In vivo characterization of the liver fat (1)H MR spectrum. NMR in biomedicine 2011; 24: 784 – 790
30 *Hernando D*, *Kuhn JP*, *Mensel B et al.* R_2^* estimation using "in-phase" echoes in the presence of fat: the effects of complex spectrum of fat. JMRI 2013; 37: 717 – 726

31 *Christoforidis A*, *Perifanis V*, *Spanos G et al.* MRI assessment of liver iron content in thalassamic patients with three different protocols: comparisons and correlations. European journal of haematology 2009; 82: 388 – 392

32 *Garbowski MW*, *Carpenter JP*, *Smith G et al.* Biopsy-based calibration of T_2^* magnetic resonance for estimation of liver iron concentration and comparison with R_2 Ferriscan. Journal of Cardiovascular Magnetic Resonance 2014; 16: 40

33 *Hankins JS*, *McCarville MB*, *Loeffler RB et al.* R_2^* magnetic resonance imaging of the liver in patients with iron overload. Blood 2009; 113: 4853 – 4855

34 *McCarville MB*, *Hillenbrand CM*, *Loeffler RB et al.* Comparison of whole liver and small region-of-interest measurements of MRI liver R_2^* in children with iron overload. Pediatric radiology 2010; 40: 1360 – 1367

35 *Virtanen JM*, *Komu ME*, *Parkkola RK.* Quantitative liver iron measurement by magnetic resonance imaging: in vitro and in vivo assessment of the liver to muscle signal intensity and the R_2^* methods. Magnetic resonance imaging 2008; 26: 1175 – 1182

36 *Henninger B*, *Zoller H*, *Rauch S et al.* R_2^* relaxometry for the quantification of hepatic iron overload: biopsy-based calibration and comparison with the literature. Fortschr Röntgenstr 2015; 187: 472 – 479

37 *Krafft AJ*, *Loeffler RB*, *Song R et al.* Does fat suppression via chemically selective saturation affect R_2^*-MRI for transfusional iron overload assessment? A clinical evaluation at 1.5T and 3T. MRM 2015; DOI: 10.1002/mrm.25868

38 *Henninger B*, *Kremser C*, *Rauch S et al.* Evaluation of liver fat in the presence of iron with MRI using T_2^* correction: a clinical approach. European radiology 2013; 23: 1643 – 1649

39 *Kuhn JP*, *Hernando D*, *Munoz del Rio A et al.* Effect of multipeak spectral modeling of fat for liver iron and fat quantification: correlation of biopsy with MR imaging results. Radiology 2012; 265: 133 – 142

40 *Ghugre NR*, *Doyle EK*, *Storey P et al.* Relaxivity-iron calibration in hepatic iron overload: Predictions of a Monte Carlo model. MRM 2015; 74: 879 – 883

41 *Juchems MS*, *Cario H*, *Schmid M et al.* Liver iron content determined by MRI: spin-echo vs. gradient-echo. Fortschr Röntgenstr 2012; 184: 427 – 431

42 *Verlhac S*, *Morel M*, *Bernaudin F et al.* Liver iron overload assessment by MRI R_2^* relaxometry in highly transfused pediatric patients: an agreement and reproducibility study. Diagnostic and interventional imaging 2015; 96: 259 – 264

43 *Rose C*, *Vandevenne P*, *Bourgeois E et al.* Liver iron content assessment by routine and simple magnetic resonance imaging procedure in highly transfused patients. European journal of haematology 2006; 77: 145 – 149

44 *Wunderlich AP*, *Cario H*, *Bommer M et al.* MRI-Based Liver Iron Content Determination at 3T in Regularly Transfused Patients by Signal Intensity Ratio Using an Alternative Analysis Approach Based on R_2^* Theory. Fortschr Rontgenstr 2016; 188: 846 – 852

45 *Wang ZJ*, *Fischer R*, *Chu Z et al.* Assessment of cardiac iron by MRI susceptometry and R_2^* in patients with thalassemia. Magnetic resonance imaging 2010; 28: 363 – 371

46 *Hernando D*, *Cook RJ*, *Diamond C et al.* Magnetic susceptibility as a B0 field strength independent MRI biomarker of liver iron overload. MRM 2013; 70: 648 – 656

47 *Jensen JH*, *Chandra R.* Theory of nonexponential NMR signal decay in liver with iron overload or superparamagnetic iron oxide particles. MRM 2002; 47: 1131 – 1138

48 *Jensen JH*, *Tang H*, *Tosti CL et al.* Separate MRI quantification of dispersed (ferritin-like) and aggregated (hemosiderin-like) storage iron. MRM 2010; 63: 1201 – 1209

49 *Tang H*, *Jensen JH*, *Sammet CL et al.* MR characterization of hepatic storage iron in transfusional iron overload. JMRI 2014; 39: 307 – 316

50 *Wood JC*, *Zhang P*, *Rienhoff H et al.* Liver MRI is more precise than liver biopsy for assessing total body iron balance: a comparison of MRI relaxometry with simulated liver biopsy results. Magnetic resonance imaging 2015; 33: 761 – 767